Engineering Structures 275 (2023) 114968

Contents lists available at ScienceDirect

Engineering Structures

journal homepage: www.elsevier.com/locate/engstruct

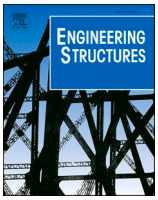

Physics-informed long short-term memory networks for response prediction of a wind-excited flexible structure

Li-Wei Tsai , Alice Alipour *

Department of Civil, Construction and Environmental Engineering, Iowa State University, Ames, IA 50011, United States

ARTICLE INFO

Keywords:
Flexible structures
Wind-induced response
Long-term monitoring
Long short-term memory

ABSTRACT

Slender and flexible infrastructures such as sign supports, cantilever traffic signal structures and high mast lighting towers are sensitive to wind force and were reported to have fatigue-related issues due to the large-amplitude vibrations throughout thier life. Simulating wind-induced structural response can be an important step to evaluate their fatigue life and reliability. However, wind simulations are usually quite complicated. A comprehensive wind force model was usually developed by conducting multiple wind tunnel tests. However, due to the high cost of wind tunnel tests and the limitation of a wind tunnel, aerodynamic and aeroelastic coefficients were usually extracted only at certain wind speeds and wind directions. Interpolation or extrapolation methods were commonly used when coefficients were not available, which makes the simulation result questionable. In this study, a methodology was proposed to simulate wind-induced structural response with lower costs. The proposed method uses monitoring data in the field to develop long short-term memory (LSTM) networks. In training LSTM networks, only the monitoring data in regular wind condition was used. However, the trained LSTM network can still predict the wind-induced response in high and extreme wind conditions observed during the monitoring of the structure. The proposed method can be useful when simulating wind-induced structural response in a wide range of wind speeds and can be widely used on other structures suspected of having fatigue damage due to wind-induced vibrations.

1. Introduction

Slender and flexible structures such as sign supports, cantilever traffic signal structures and high mast lighting towers are very sensitive to wind force. Long-term wind-induced vibrations of these structures eventually results in fatigue damage on locations with high stress concentration such as base-plate-to-tube connections or mast-arm-to-pole connections. Fatigue failures of traffic signal support structures and high mast lighting towers have been reported across the United States over the past 20 years [1,9,12,16,35,48], which highlights the need to study their wind-induced behavior, fatigue assessment and reliability analysis.

Simulating wind-induced structural response can be an important first step for evaluating fatigue damage and predicting fatigue life and reliability of these wind-excited structures. Physics-based models were usually developed to simulate wind-induced structural response. Generally, wind simulation requires modeling the structure and the wind force on the structure. Commonly, structures can be modeled by mathematical equations of motion [36,37] or detailed finite element models [13,14,42,44,56]. However, modeling wind force on a structure can be complicated. Wind force on a structure can vary due to many factors such as turbulence intensity, aerodynamic shape and surface roughness which are all difficult to be formulated. The different assemblies on these structures such as luminaires and traffic lights make the modeling of the wind force even more difficult. A simplified wind force equation was used in modeling the wind force on high mast lighting towers to simulate structural response [36,37,14,42]. A more comprehensive wind force equation was used in modeling the wind force on high mast lighting towers [35] and traffic signal structures [2,21,30], which requires aeroelastic and aerodynamic parameters of the structures. These coefficients were extracted by previous wind tunnel tests on multi-sided and circular cylinders and traffic light models [21,23,38,39,45]. It can be noticed that the traditional method in developing a comprehensive wind force model requires multiple wind tunnel tests on different components of a structure, which can be expensive. Also, due to the high cost and the wind speed limit in a wind tunnel, wind tunnel tests were usually only conducted at some specific wind speeds and wind directions. Interpolation or extrapolation

* Corresponding author.
E-mail address: alipour@iastate.edu (A. Alipour).

https://doi.org/10.1016/j.engstruct.2022.114968

Available online 16 November 2022

methods are usually used when coefficients are not available. Considering the wind in the real world can be much more turbulent, the wind-induced response simulation from a physical-based model can sometimes be questionable.

Due to the downsides of the traditional method mentioned above, other group of studies came up with using machine learning techniques to develop surrogate models in simulating structural response. Earlier research started with using machine learning techniques in simulating seismic structural response. Artificial neuron networks (ANNs) were trained and validated to be able to generate response matching the response from physics-based model of multi-story buildings such as mathematical system equations or finite element models [7,33,53–55]. In [34], a recurrent neuron network (RNN) was trained by the acceleration data recorded from previous shake table tests and validated to be able to generate precise response. Eventually, in [50], a long short-term memory (LSTM) network was trained by the acceleration data recorded from a 6-story building in San Bernardino, California during seismic events. The trained LSTM network was validated to be able to control normalized prediction error within 3%. Therefore, it has been validated that machine learning models can become accurate surrogate models in predicting real-life seismic structural response.

Comparing with seismic response, predicting wind-induced structural response can be more challenging as discussed previously. Similarly, a group of studies used machine learning techniques to replicate the simulated wind-induced response from physics-based models. For example, Wang and Wu [46] trained a LSTM network to replicate the simulated data from a multiple-degree-of-freedom (MDOF) system equation. Bani-Hani [3] trained an ANN to generate response matching the response from a MDOF system of a tall building. Xue et al. [49] used a convolutional neuron network to replicate the simulated data from a finite element model of a transmission tower. In [27], the mathematical model of a bridge deck used a more comprehensive wind force equation, which included aeroelastic and aerodynamic parameters, and a LSTM network was trained by the simulated data and was successfully validated. Hareendran and Alipour [17] showed that the LSTM could predict the nonlinear response of wind-excited tall buildings and Micheli et al. [31] provided the applicability of a series of different techniques in the context of tall building design. At this point, these studies have presented that machine learning models are able to replace physics-based models to simulate wind-induced response with higher efficiency.

In the next stage, a number of studies started to train machine learning models by the response data recorded from wind tunnel tests. For example, Dongmei et al. [11] trained and validated an ANN by the wind pressure data from a scaled model of a high-rise building in wind tunnel tests. Oh et al. [32] trained and validated a CNN by the strain data from a scaled model of a 5-story building in wind tunnel tests. Hu and Kwok [20] used multiple machine learning algorithm to predict wind pressure on circular cylinder models. Lin et al. [29] compared 5 different machine learning models in predicting the crosswind vibrations of rectangular cylinder models and also studied the influence of the side ratios to the crosswind response. These studies have shown machine learning models have the potentials in predicting wind-induced response of real structures.

Finally, machine learning models were trained by the monitoring data from real structures to study specific wind-induced structural behaviors such as vortex-induced or buffeting-induced vibrations and to predict wind-induced structural response. Vortex-induced vibrations were commonly observed on long-span bridges or slender vertical structures. Li et al. [24] and Lim et al. [28] have conducted long-term monitoring on long-span bridges and a tall building. They proposed cluster analysis and supervised machine learning techniques to identify vortex-induced vibrations from the long-term monitoring data. Li et al. [25] later used decision tree learning and support vector regression to predict the vertical displacement during vortex-induced vibrations. Wind-induced vibrations in along-wind direction happen almost all the time and are basically excited by drag and buffeting wind forces. Only a few studies focused on predicting buffeting-induced structural response using machine learning techniques. In [5], long-term monitoring data from a long-span bridge in Norway was used to train multilayer perceptron and support vector regression models to predict buffeting-induced response. The predictions from the two models were compared with the response generated by buffeting theory. The result showed the machine learning models could make more accurate wind-induced response. In [26], a LSTM network was trained by the monitoring data from a bridge in China to predict the buffeting-induced displacement of the bridge deck. The predictions from the trained model and a finite element model were compared. The result also showed the trained model can better predict the wind-induced structural response.

These studies successfully used machine learning techniques to move wind-induced response predictions from lab theory to practical engineering. However, a few research gaps could be identified. First, it seems training data and testing data were not well explained, therefore, it's difficult to understand the performance and the limitation of the trained machine learning models. Second, the models were trained and tested in a specific range of wind speed (mostly less than 25 m/s). The performance of the trained models at wind speeds higher than the training data is still unknown. Also, the models were developed by only the monitoring data in the field. Therefore, it is possible that the models can only learn the wind-induced behavior at the wind speeds of the training data. The predictions beyond the training wind speeds might be questionable.

This study took advantage of the available monitoring data for a wind-induced cantilever traffic signal structure (also categorized as a flexible structure) to train a special class of RNNs. The traffic signal structure is located in Ames, Iowa and was monitored for over a year. Sensors including an anemometer and accelerometers were installed to record wind data and wind-induced acceleration at the tip of the mast arm, respectively. To address the identified gaps, the proposed method used two long short-term memory (LSTM) networks to predict the wind-induced structural response. The first LSTM network was trained as the mathematical model of the structure to faster simulate more and longer wind-induced response, which possesses the general understanding of wind-induced behaviors of the structure. The second LSTM used the simulated wind-induced response and the monitoring wind data to predict the monitoring wind-induced data. Therefore, the trained model will be physics-informed. In this study, LSTM networks were trained by the monitoring data in regular wind condition. The trained LSTM networks were then tested by unseen monitoring data in regular and high wind conditions. It is worth to mention that the monitoring data during the 2020 derecho in Iowa, which was categorized as an inland hurricane with sustained wind speeds of more than 130 mph, was also used in testing the trained LSTM networks. The trained LSTM was very well able to predict the amplitude of the wind-induced acceleration in regular, high, and extreme wind conditions. This study is valuable since only a few sensors were used in the field and only the monitoring data in regular wind condition was used in training LSTM networks. The trained LSTM network also predicted better wind-induced response than the mathematical model generated based on traditional methods.

This paper is organized as follows: Section 2 describes the monitored traffic signal structure and the instrumentation plan. Section 3 explained the proposed method for predicting wind-induced response by using machine learning approaches and monitoring data in the field. Section 4 presents the results of the predicted wind-induced response and the evaluation of the accuracy of the trained LSTM networks. Section 5 concludes and discusses the findings of this study.

2. Monitored traffic signal structure

Previously, a cantilevered traffic-signal structure in Ames, Iowa, was selected for long-term monitoring to study the wind-induced behavior [2,43]. The structure was comprised of a 7.62 m vertical pole, a 20.42 m

curved mast arm, and three vertical traffic lights attached to the mast arm. The mast arm was welded to an arm base plate bolted to another plate on the vertical pole. Dimensional details are shown in Fig. 1 and the orientation of the selected structure is shown in Fig. 2. Note that the three vertical traffic lights face to the east. Other details on the structure can be found in [2,43].

During the long-term monitoring, sensors including an anemometer and two accelerometers were installed on the selected traffic signal structure. The anemometer was installed at the top of the vertical pole. It can record both wind direction and wind speed. Wind direction was measured in degrees (0° ~ 360°) with 0° representing a north wind (wind from north blowing south), 90° an east wind, 180° a south wind, and 270° a west wind. Wind speed was measured in mph. Two accelerometers were installed at the tip of the mast arm to record the accelerations in in-plane (vertical) and out-of-plane (horizontal) directions respectively. See the instrumentation plan in Fig. 3. Details of each sensor and data acquisition device can be found in [43]. The monitoring data was used to train and test the ANN in this study.

3. Methodology

3.1. Long short-term memory network

Before explaining the proposed methodology, a brief introduction of long short-term memory network and the reason of using it in this study were provided in the following.

Recurrent neuron network (RNN) has been widely used on sequence data-related tasks, such as language modeling and speech recognition [15,40]. The hidden states in an RNN allows it to remember previous outputs and to be able to learn the relation of the data between each time step, see Fig. 4 (a). However, RNN can only pass the information across very limited time steps because of the problem of vanishing and exploding gradients [4,22]. Hochreiter & Schmidhuber [19] proposed long short-term memory network to overcome this issue.

The schematic of a standard LSTM network is shown in Fig. 4(b). In each LSTM cell, cell state (c_i) can pass long term memory. At the same time, forget gate is able to remove out-of-date information from the cell state by using the logistic sigmoid function and multiplication operation. The logistic sigmoid function has a range between 0 and 1, which indicates forget gate is able to fully forget or memorize the previous cell state. Input gate and *tanh* gate are used to add new information to the cell state from the hidden state and the current input data. Output gate combines the cell state, the hidden state and the input data to decide the output information. Note that in Fig. 4(b), the output (y_i) can be the same as the hidden state (h_i), however, a fully connected layer is usually used to convert the hidden state to an output with a desired dimension. The details of the proposed methodology will be given in the following subsections.

3.2. Proposed method for predicting wind-induced structural response

At the beginning, a mathematical model for the monitored traffic signal structure was built to simulate its wind-induced response. The simulated response has a fair accuracy when comparing to the monitoring response. However, it was noticed that the mathematical model sometimes showed too conservative results. It can be explained that some uncertainties of wind-induced structural behavior are difficult to formulate and caused the discrepancy between simulated response and monitoring data.

The first idea was to train a LSTM network to map monitoring wind data to monitoring wind-induced response. However, at higher wind speeds the error between predictions and reference was high and the test results were not good enough. This is obviously expected since the monitoring data used was for lower wind speeds. Furthermore, the anemometer installed in the field could only record 2-dimentional wind data, which are wind speed and wind direction. It can be difficult to train a LSTM network to learn the wind-induced structural behavior by only 2-dimensional wind speed and wind direction data.

Therefore, the LSTM-WR was modified in such a way that it can use wind data and simulated wind-induced response from the mathematical model as inputs and output revised wind-induced response closer to the field monitoring data. Therefore, LSTM-WR is going to learn those uncertainties that the mathematical model is not able to cover and make up the discrepancy between the simulated response and the monitoring data. Training LSTM-WR needs a large database. Large database of wind and wind-induced structural response were recorded in the field. However, generating large database of simulated results from the mathematical model could be an issue. Previously, different types of machine learning models have shown the success in replicating the simulated structural response from mathematical models with a much higher efficiency. Therefore, the authors developed another LSTM network (called LSTM-Math i) to replace the mathematical model to faster generate large amounts of simulated structural response.

Fig. 5 shows the proposed methodology to develop LSTM networks

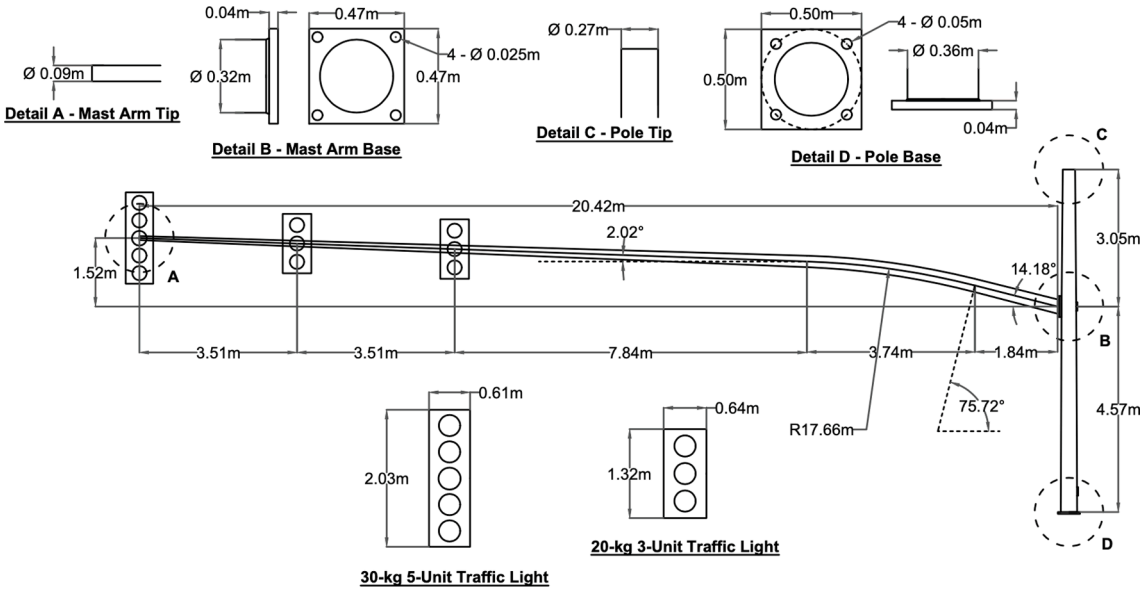

Fig. 1. Detailed dimensions of the monitored traffic signal structure, located in Ames, IA.

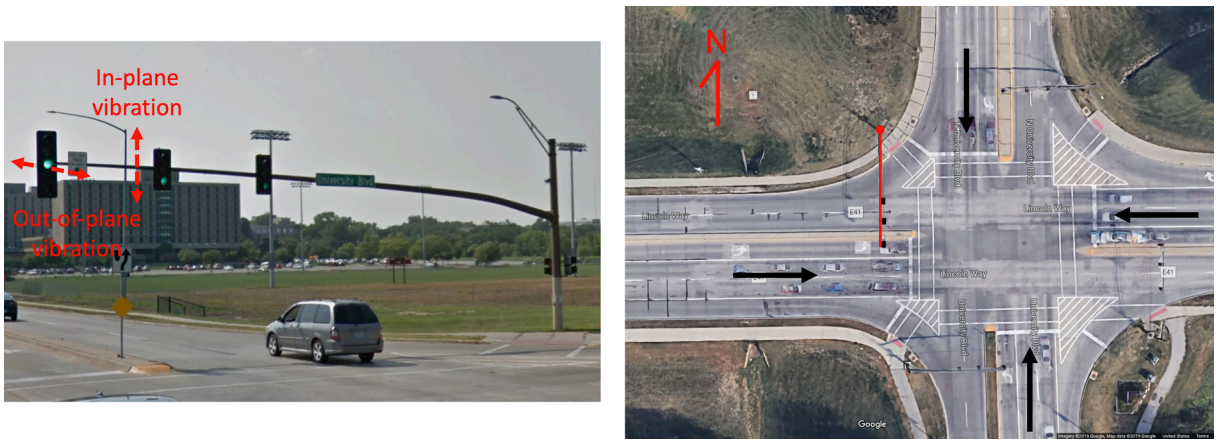

Fig. 2. The location of the monitored traffic signal structure and the definitions of in-plane and out-of-plane vibrations.

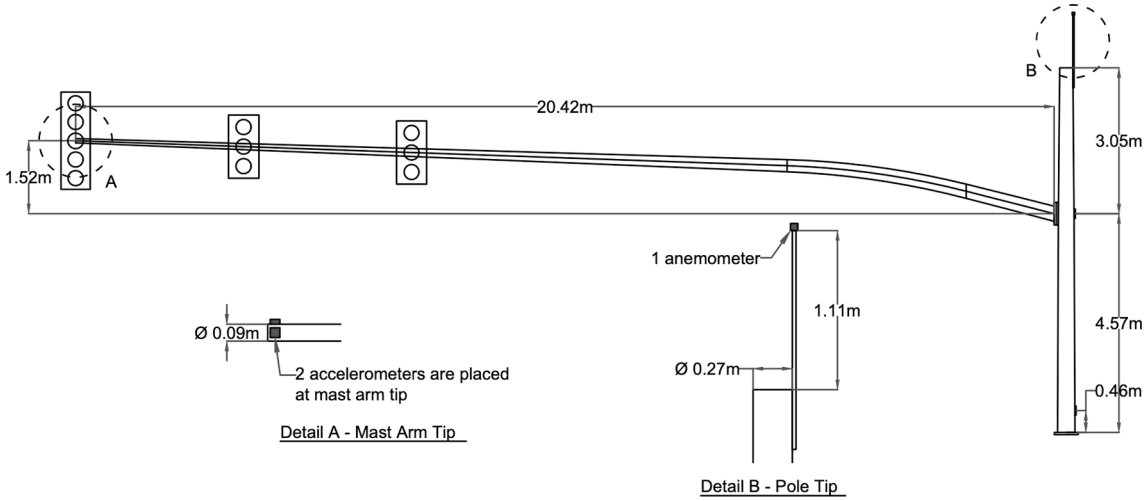

Fig. 3. Instrumentation plan of sensors.

for predicting wind-induced structural response. It can be explained in the following steps:

Step 1: The proposed method starts with building a mathematical model of the monitored traffic signal structure and optimizing the aerodynamic and aeroelastic parameters in the mathematical model.
Step 2: The optimized mathematical model will be used to generate simulated wind-induced response which provides physical meanings and also helps the training of the LSTM network faster. However, generating large amounts of simulation data by using the mathematical model is time-consuming. Therefore, a LSTM network called LSTM-Math is trained to replace the mathematical model.
Step 3: Another LSTM network called LSTM-WR will be trained by taking the monitoring wind data and the simulated response from LSTM-Math as inputs and the monitoring wind-induced response as reference. The trained LSTM-WR will eventually be used to predict the wind-induced structural response.

Details of each step in the proposed frame will be given in the following subsections.

3.3. Step 1: Mathematical model and optimization

This subsection explained the details of Step 1. The mathematical model of the monitored traffic signal structure has been developed in [2]. It was written as a system matrix equation of motion, Eq. (1).

$$M_{11\times11}\ddot{q} + C_{11\times11}\dot{q} + K_{11\times11}q = \boldsymbol{Q}_{11\times1} \tag{1}$$

where M is the mass matrix, C is the damping matrix, K is the stiffness matrix, Q is the generalized force matrix and q is the generalized coordinates.

In the mathematical model, a total of 11 mode shapes were used to describe the motion of the traffic signal structure which are corresponding to 11 generalized coordinates. The in-plane and out-of-plane vibrations of the mast arm used 4 mode shapes respectively, and the in-plane, out-of-plane and twisting motions of the vertical pole used 1 mode shape respectively.

Pluck tests were conducted in the field to extract the damping ratios of the first four modes and the damping ratios of the rest of the modes were assumed to be 0.5%. The damping matrix was derived by superimposing the modal damping matrices.

Wind force was only considered the wind force on the mast arm which includes the drag and buffeting force on the traffic lights (F_b^l) and the mast arm (F_b^a) and the self-excited force on the traffic lights (F_{se}^l) and the mast arm (F_{se}^a), see Eq. (2). The generalized force matrix was then derived by virtual work principle. Details of the model derivation can be found in [2].

$$F_b^a(x,t) = \frac{1}{2}\rho_{air}U^2 C_{D_{arm}} D_{arm}(x) \tag{2}$$

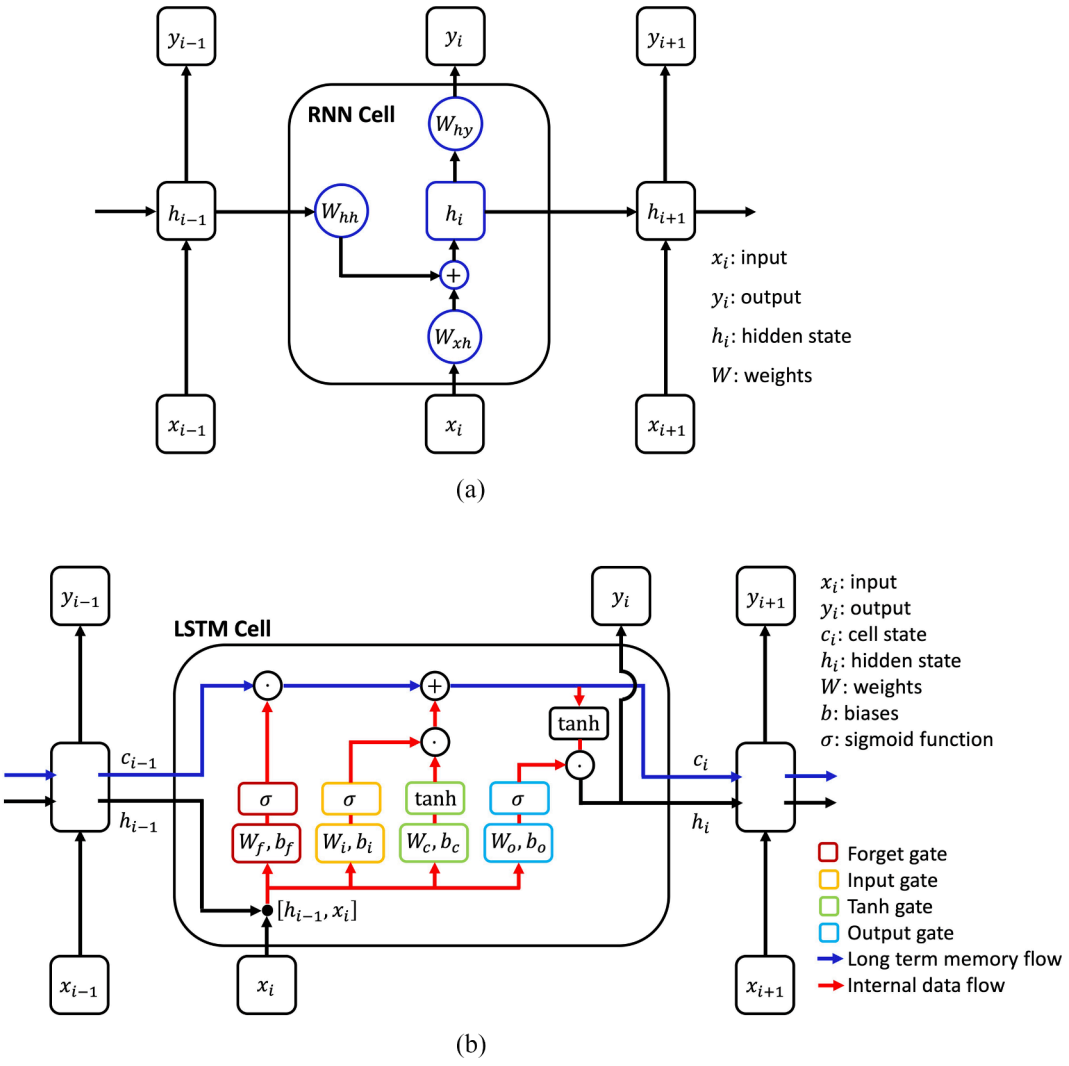

Fig. 4. Schematics of (a) a standard RNN and (b) a standard LSTM network.

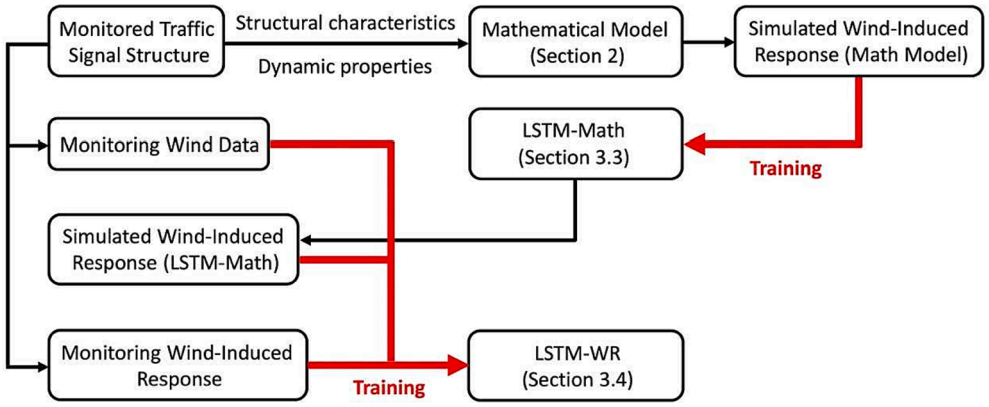

Fig. 5. Proposed methodology to develop a LSTM network to predict wind-induced structural response.

$$F_{se}^{a}X(x,t) = \frac{1}{2}\rho_{air}U^2 D_{arm}(x)\left[\frac{KP_5^*}{U}\dot{v}^a + \frac{KP_1^*}{U}\dot{w}^a + \frac{K^2P_6^*}{D_{arm}}v^a + \frac{K^2P_4^*}{D_{arm}}w^a\right]$$

$$F_{se}^{a}Y(x,t) = \frac{1}{2}\rho_{air}U^2 D_{arm}(x)\left[\frac{KH_1^*}{U}\dot{v}^a + \frac{KH_5^*}{U}\dot{w}^a + \frac{K^2H_4^*}{D_{arm}}v^a + \frac{K^2H_6^*}{D_{arm}}w^a\right]$$

$$F_b^l(t) = \frac{1}{2}\rho_{air}U^2 C_{D_{light}}A_{light}$$

$$F_{se}^{l}X(t) = \frac{1}{2}\rho_{air}U^2 A_{light}\left[\frac{KP_5^*}{U}\dot{v}^a + \frac{KP_1^*}{U}\dot{w}^a + \frac{K^2P_6^*}{D_{light}}v^a + \frac{K^2P_4^*}{D_{light}}w^a\right]\Bigg|_{x=L_1,L_2,L_3}$$

$$F_{se}^{l}Y(t)=\frac{1}{2}\rho_{air}U^{2}A_{light}\left[\frac{KH_{1}^{*}}{U}\dot{v}^{a}+\frac{KH_{5}^{*}}{U}\dot{w}^{a}+\frac{K^{2}H_{4}^{*}}{D_{light}}v^{a}+\frac{K^{2}H_{6}^{*}}{D_{light}}w^{a}\right]\Bigg|_{x=L_{1},L_{2},L_{3}}$$

where ρ_{air} is the air density, $C_{D_{arm}}$ and $C_{D_{light}}$ are the drag coefficients of the mast arm and traffic lights respectively, D_{arm} is the diameter of the mast arm, A_{light} is the projected area of traffic lights, and H^{*} and P^{*} are the flutter derivatives.

In this study, the mathematical model was further optimized by using the monitoring data. The idea is to find the optimal values of the aeroelastic and aerodynamic parameters in wind force equations to generate wind-induced response close to the monitoring data. The initial guess of these parameters was selected as some reasonable values based on the prior knowledge. For example, the drag coefficients of a flat plate and a circular cylinder were used as the initial guess of the drag coefficients of the traffic light and the mast arm. SThe optimization was implemented in MATLAB using gradient-based built-in functions. The cost function was defined as the root mean square error between the simulated response and the monitoring response. Fig. 6 shows the simulated acceleration at the mast arm tip by the optimized mathematical model and the monitoring acceleration data at the mast arm tip. The optimized mathematical model is able to simulate the wind-induced acceleration with similar amplitudes to the monitoring acceleration data in both out-of-plane and in-plane directions.

3.4. Step 2: LSTM network for the mathematical model

The optimized mathematical model has shown a fair accuracy in simulating the wind-induced response. However, running dynamic simulation by solving the differential matrix equation of motion is time-consuming. Furthermore, knowledge of the structural dynamics of structure and initial values for aerodynamic coefficients is not always available. To address these issues, an LSTM network called LSTM-Math was trained as the surrogate model of the optimized mathematical model.

The mathematical model takes only the wind speed perpendicular to the mast arm as the effective wind speed, therefore, monitoring wind speed (V) and wind direction (θ) data were converted to perpendicular wind speed data ($U_{\perp}$).

$$U_{\perp}=V\times sin(\theta) \tag{3}$$

The mathematical model then took the perpendicular wind speed data as the input to generate the simulated wind-induced response. Fig. 7 shows the schematic of LSTM-Math. LSTM-Math consists of multiple LSTM layers and fully connected layers. The input data (x_i) of LSTM-Math was defined as the perpendicular wind speed data of the current moment and the past few seconds. The output data (y_i) was the wind-induced response, which should be as close as possible to the simulated wind-induced response of the mathematical model.

3.5. Step 3: LSTM network for predicting wind-induced response

After LSTM-Math is trained and validated, it can be used to faster simulate more and longer duration of wind-induced responses. The optimized mathematical model has shown a fair accuracy in simulating wind-induced responses. To further enhance the prediction accuracy, a LSTM network called LSTM-WR was trained to eventually generate accurate wind-induced response.

The schematic of LSTM-WR is shown in Fig. 8. LSTM-WR consists of multiple LSTM layers, multiple fully connected layers and a drop-out layer. The input (x_i) of LSTM-WR was defined as wind speed (V), wind direction (θ), perpendicular wind speed ($U_{\perp}$), parallel wind speed ($U_{\parallel}$) and the simulated response ($\tilde{y}$) from LSTM-Math of the current moment and the past few seconds.

$$U_{\perp}=V\times\sin(\theta),U_{\parallel}=V\times\cos(\theta) \tag{4}$$

This can be explained as follows. The anemometer installed in the field can only record two-dimensional wind speed and wind direction. Therefore, there are only two types of input data, wind speed and wind direction. Considering the complexity of wind-induced structural response, other types of input data were derived from the existing wind data to help LSTM-WR to learn more complex wind-induced structural behavior. In common wind force equations such as drag, buffeting and self-excited force, which were shown in Eq. (2), perpendicular wind speed is usually used with aeroelastic and aerodynamic parameters and is believed to have a strong relation with out-of-plane vibrations. Therefore, perpendicular wind speed was calculated to be one of the inputs. Also, from the previous study on traffic signal structures through long-term monitoring data [43], it was observed that large amplitude out-of-plane vibrations did not always happen in the direction perpendicular to the mast arm. There was a considerable amount of large out-of-plane vibrations observed when the wind direction is parallel to the mast arm. Therefore, parallel wind speed was also calculated to be one of the inputs. Eventhough wind speed and wind direction were used to derive the perpendicular and parallel wind speeds, they could have their own meanings to the wind-induced behavior. The simulated wind-induced response from LSTM-Math was one of the inputs to provide physical meanings to LSTM-WR. Considering the asymmetric shape of a cantilever traffic signal structure and traffic lights and sign plates

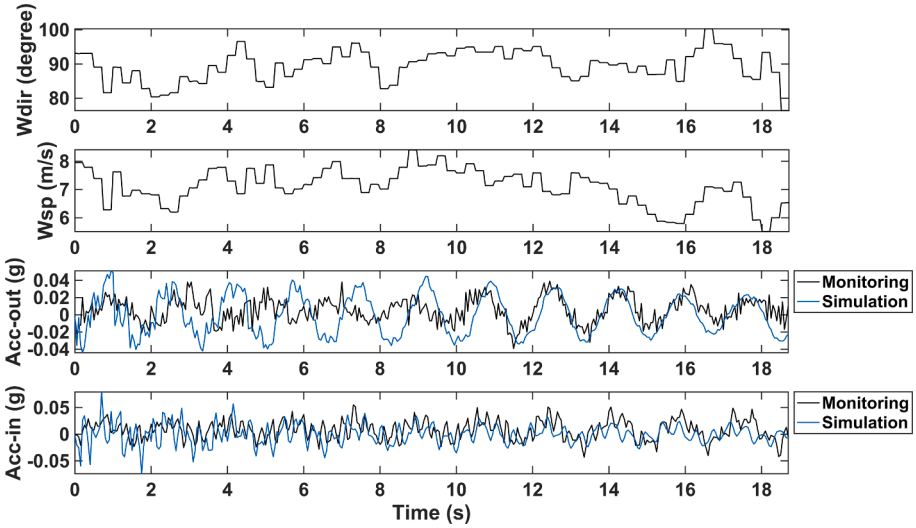

Fig. 6. Comparison of the simulated and monitored accelerations.

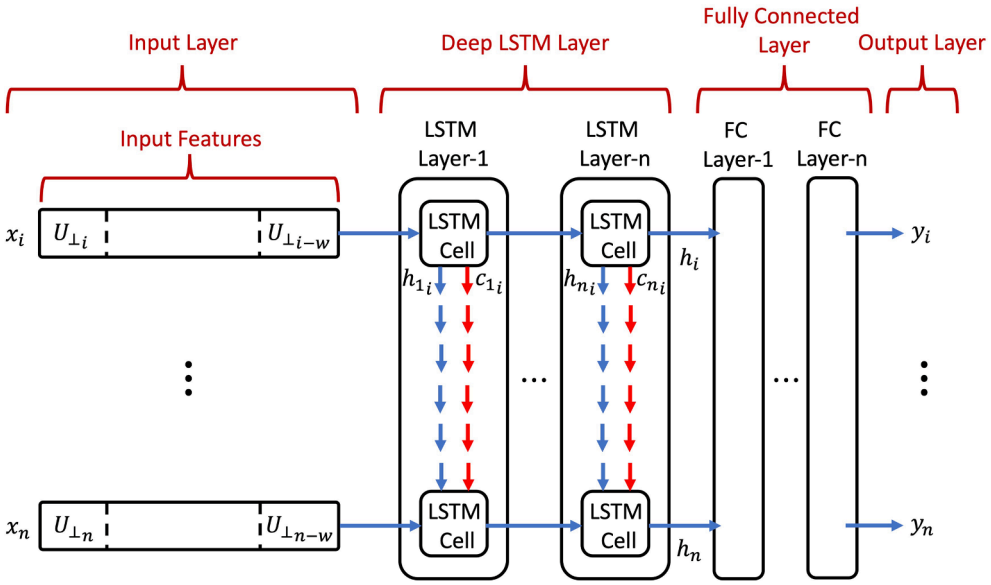

Fig. 7. Schematic of LSTM-Math.

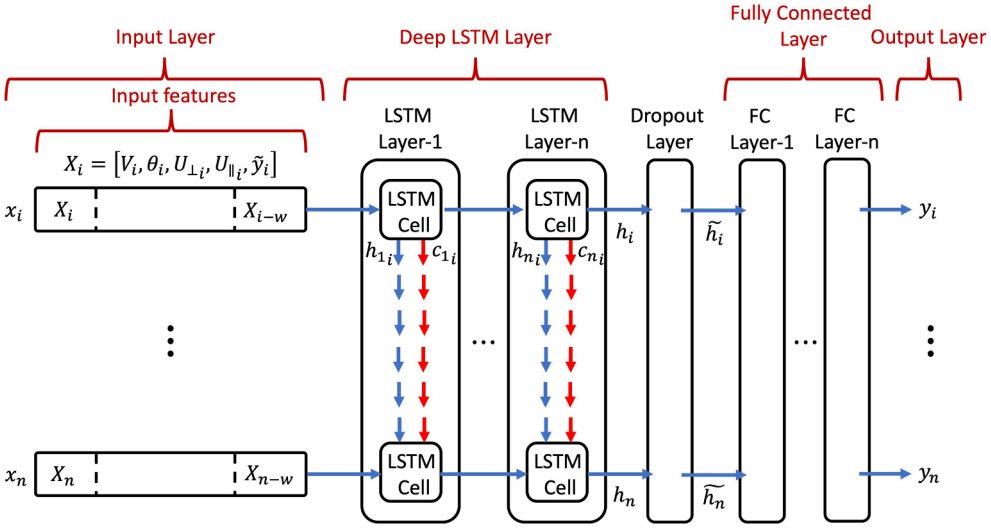

Fig. 8. Schematic of LSTM-WR.

attached on the mast arm, its wind-induced structural response can be quite complicated. Therefore, the inputs were defined as these five types of data from the current moment to the past few seconds to make the input features even more diverse.

The output (y_i) was defined as the error between the simulated wind-induced response from LSTM-Math and the monitoring wind-induced response. Finally, the predicted wind-induced response can be simply obtained by adding the output and the simulated response from LSTM-Math together. Such definition of the output is quite important because it forces LSTM-WR to generate response better than the simulated response from LSTM-Math.

4. Results

4.1. Monitoring data processing and selection

Large-amplitude wind induced vibrations are often observed on cantilever traffic signal structures. Fatigue failures of such structures in the United States have created the needs on studying its wind-induced mechanism and evaluating its fatigue life and reliability. Wind tunnel tests and field monitoring have been conducted to reveal the wind-induced mechanisms [21,23,38,39,45,7,8,10,18,41,47,48,51]. These studies finally identified several types of large-amplitude vibrations of traffic signal structures, which includes vortex- and galloping-induced vibration in across-wind direction and buffeting-induced vibration in along-wind direction.

In this study, the traffic signal structure was monitored in 2019 and 2020 inclduing during the Iowa Derecho of 2020. Using the monitoring data, the study was first focused on its wind-induced behavior and evaluating the fatigue damage due to wind-induced vibrations [43]. It was observed that a cantilever traffic signal structure with vertical traffic lights on the mast arm might have lower chances to experience vortex-induced vibrations which are in in-plane direction. Large vibrations of this type of traffic signal structures were majorly in out-of-plane direction, which are basically excited by drag and buffeting wind forces, and were believed to create fatigue damage on at the mast arm base. Therefore, in this study, the proposed methodology focused on predicting the wind-induce response in out-of-plane direction.

The monitoring data was cut into 5-min data segments. Each 5-min data segment contains wind speed data, wind direction data and out-

of-plane acceleration at the mast arm tip. A general idea is using wind speed data and wind direction data to predict out-of-plane acceleration by machine learning techniques. Considering the limited input information and the complexity of wind-induced structural response, the monitoring data was simplified and filtered in this study. First, a low-pass filter with a cut-off frequency of 0.6 Hz was applied on out-of-plane acceleration data. Therefore, out-of-plane acceleration data shows only the response of the 1st mode. Second, it is generally believed that the vibration amplitude and the wind speed should roughly be a linear correlation. Therefore, 5-second standard deviation of out-of-plane acceleration and 5-second perpendicular wind speed were calculated for each 5-min data segment and the R-squared value was calculated to evaluate its linearity, see Fig. 9. In this study, 5-min data segments with R-squared value larger than 0.3 were selected. Finally, only the 5-min data segments in regular wind condition, which was defined as the maximum wind speed lower than 17.88 m/s (40 mph), were selected in training the LSTM networks. The purpose was to demonstrate the proposed methodology only requires monitoring data in regular wind condition.

4.2. Performance of LSTM-Math

Following the procedures in Section 3, LSTM-Math was first trained to perform as the optimized mathematical model. In this study, LSTM-Math used 7 LSTM layers and 3 fully connected layers. The number of hidden states of each LSTM layers were set to 100. The input was taken as a perpendicular wind speed history from the current moment to 3 s ago. The time step interval was 0.1 s, therefore, the number of input features was 30. The output was the out-of-plane acceleration at the tip of the mast arm.

In the training of LSTM-Math, 400 of 1-min data were used. Each 1-min data consists of 1-min perpendicular wind speed data and 1-min out-of-plane acceleration data which is simulated by the optimized mathematical model. The minimum batch size was set to 5 and the training was completed by 200 epochs. In the test of LSTM-Math, 2000 of unseen 2-min data were used. Similarly, each 2-min data consists of 2-min perpendicular wind speed data and 2-min out-of-plane acceleration data which is simulated by the mathematical model.

To evaluate the accuracy of LSTM-Math, normalized root mean square error (NRMSE) was calculated for each 2-min test data, Equation (5). The root mean square error was normalized by the difference between the maximum and the minimum monitoring accelerations in 2 min. Fig. 10 shows the distribution of the NRMSE values. Since the distribution of the NRMSE values was unknown, Kernel distribution was used to approximate the probability density function (PDF) of the NRMSE values. As shown in Fig. 10, all the test results showed a NRMSE value lower than 0.1 and 50% of the test results have a NRMSE value lower than 0.03. Fig. 11 shows a test result with a NRMSE value of 0.04. Therefore, LSTM-Math is able to replace the mathematical model to simulate wind-induce response.

$$NRMSE = \sqrt{\frac{\sum_{i=1}^{N}(y_i - \hat{y}_i)}{N}} \Big/ \left(\max(\hat{y}_i) - \min(\hat{y}_i)\right) \quad (5)$$

where y_i is the data generated by LSTM-Math and $\hat{y}_i$ is the data generated by the mathematical model.

To evaluate the efficiency of LSTM-Math, different lengths of simulation data were generated by the mathematical model and LSTM-Math, and their computational times were compared, see Fig. 12. The computational time for generating simulated wind-induced response decreased dramatically by using LSTM-Math. The speed of generating simulation data by LSTM-Math can be around 300 times faster than the mathematical model.

4.3. Performance of LSTM-WR

Following the procedures in Section 3, the next step is to train LSTM-WR and finally use it to predict the wind-induced response.

In this study, LSTM-WR used 11 LSTM layers, 1 dropout layer and 4 fully connected layers. The number of hidden states of each LSTM layers was set to 100. The input is taken as wind direction, wind speed, perpendicular wind speed, parallel wind speed and simulated out-of-plane acceleration by LSTM-Math from the current moment to 15 s ago. The time step interval was 1 s, therefore, the number of input features was 75. The output is the error between the simulated out-of-plane acceleration and the monitoring out-of-plane acceleration. Later, the prediction of the monitoring out-of-plane acceleration can be obtained by simply subtracting the predicted error from the simulated out-of-plane acceleration.

In the training of LSTM-WR, 400 of 5-min data were used. Each 5-min data consists of 5-min wind data, 5-min simulated out-of-plane acceleration data and 5-min monitoring out-of-plane acceleration data. As mentioned in Section 4.1, the monitoring out-of-plane acceleration data was low-pass filtered and the cut-off frequency was set to 0.6 Hz. The minimum batch size was set to 5 and the training was completed by 200 epochs.

In the test of LSTM-WR, 2000 of 5-min data in regular wind condition were first used. Similarly, each 5-min data consists of 5-min wind data, 5-min simulated out-of-plane acceleration data and 5-min monitoring out-of-plane acceleration data. Fig. 13 shows the prediction of the out-of-plane acceleration from one of the 5-min test data. As shown in Fig. 13, LSTM-WR is able to correct the simulated out-of-plane acceleration and make a prediction closer to the monitoring out-of-plane acceleration.

To evaluate the accuracy of LSTM-WR in regular wind condition, the NRMSE value was calculated for each 5-min test data. Similar to Equation (5), the root mean square error was normalized by the difference between the maximum and the minimum monitoring acceleration in 5 min. Fig. 14 shows the distribution of the NRMSE values. It can be seen that almost all the 5-min prediction data have a NRMSE value lower than 0.2 and around 50% of the 5-min prediction data have a NRMSE value lower than 0.15. Fig. 13 shows a test result with a NRMSE value of 0.14. It can be noticed that predictions were not always accurate, however, the predicted acceleration amplitude mostly matched the monitoring data. The NRMSE value was also calculated for each 5-min out-of-plane acceleration data generated by LSTM-Math. It can be observed that LSTM-WR has largely improved LSTM-Math in predicting the monitoring wind-induced response.

Next, LSTM-WR was tested by 300 of 5-min data in high and extreme wind conditions (the maximum wind speed larger than 40 mph). The NRMSE value was again calculated for each test data. Fig. 15 shows the NRMSE distribution of LSTM-WR in high and extreme wind conditions. It can be noticed the accuracy of LSTM-WR in high and extreme wind conditions is about the same as in regular wind condition. Almost all the test results have a NRMSE value lower than 0.2 and about 50% of the test

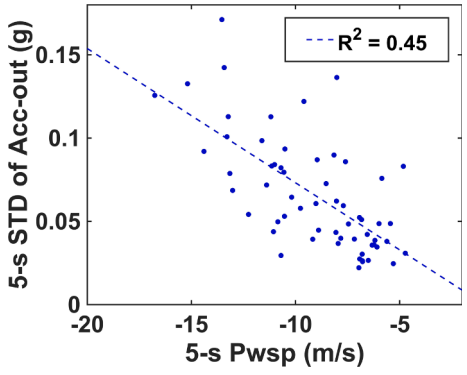

Fig. 9. 5-s perpendicular wind speed vs. 5-s standard deviation of out-of-plane acceleration.

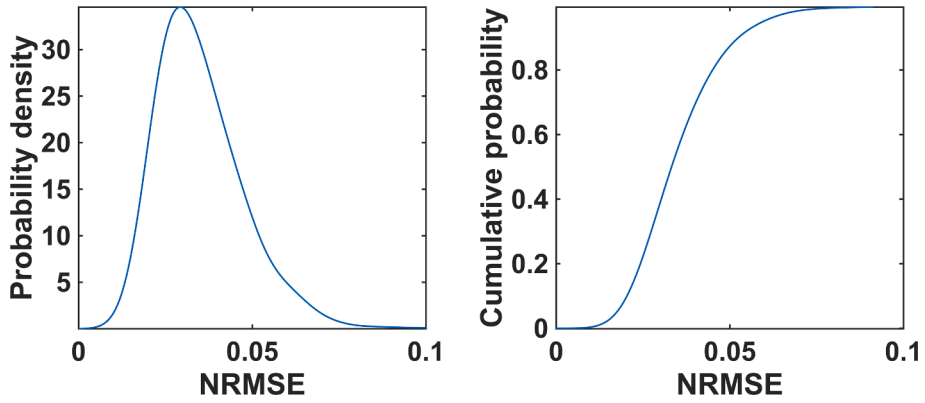

Fig. 10. (a) The PDF and (b) the CDF of NRMSE values.

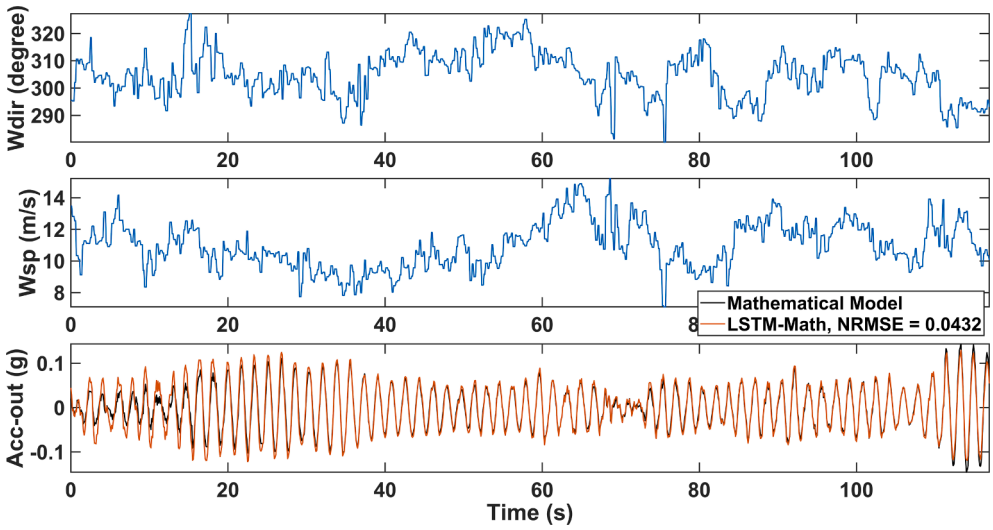

Fig. 11. LSTM-Math tested by a 2-min data.

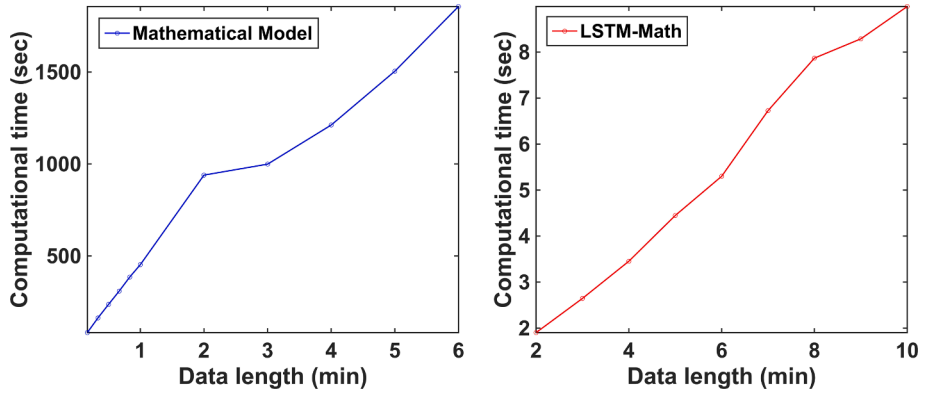

Fig. 12. Computational time of (a) the mathematical model and (b) LSTM-Math.

results have a NRMSE value lower than 0.14. Fig. 16 shows a test result with a NRMSE of 0.14. It can be seen that LSTM-WR is able to well predict the acceleration amplitude in high wind condition.

The instrumentation of the structure was fully operational when the August 10, 2020 derecho of Iowa occurred. The derecho caused notably high wind speeds of up to 126 mph recorded in Iowa, with post-damage assessments of up to 140 mph in some places. The instrumented structure provided a large opportunity as the sensors were working properly at the time, and wind-induced response was recorded. These data were also used to test LSTM-WR to check the validity of the trained model in predicting out-of-plane acceleration in extreme wind condition. Fig. 17 shows one result of LSTM-WR tested by a 5-min data during the derecho. It can be first seen that the simulation from LSTM-Math (the mathematical model) was too conservative in extreme wind condition. This indicated that the mathematical model built by the identified parameters from wind tunnel tests was not accurate in extreme wind condition. This is attributed to the fact that there are many uncertainties in high or extreme wind conditions which are difficult to be formulated. However,

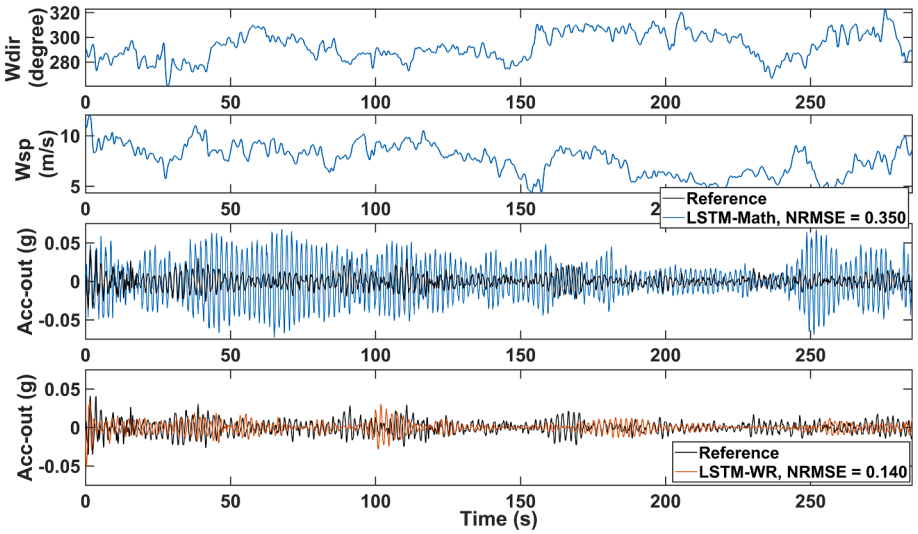

Fig. 13. LSTM-WR tested by a 5-min data in regular wind condition.

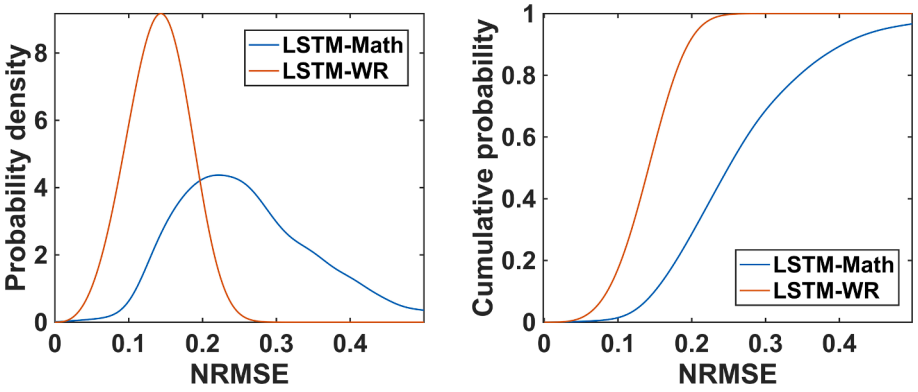

Fig. 14. NRMSE distribution of LSTM-WR in regular wind condition.

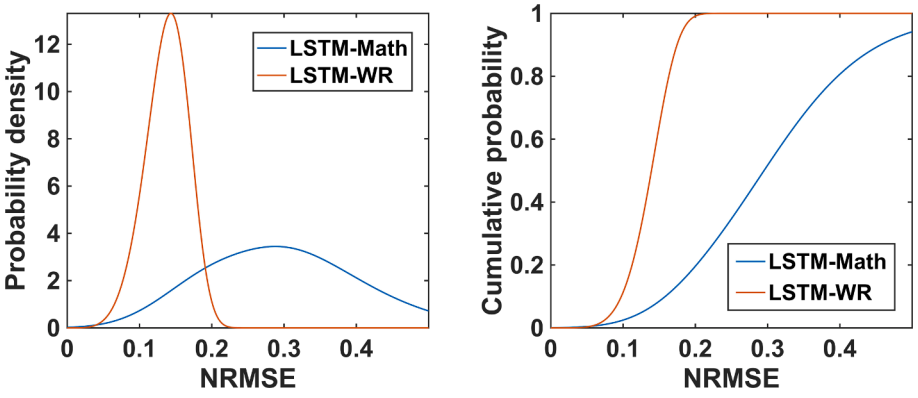

Fig. 15. NRMSE distribution of LSTM-WR in high and extreme wind conditions.

the LSTM-WR trained by the data in regular wind condition can very well predict the acceleration amplitude in extreme wind condition.

As a final step, all the test data and prediction data were cut into 1-min data segments. The maximum wind speed and the maximum amplitude of out-of-plane acceleration were calculated for each 1-min data segment and plotted on Fig. 18. An exponential function, Eq. (6), was used to approximate the upper and lower bounds of the maximum amplitude of the monitoring data at different 1-min maximum wind speeds. It was calculated there were 94% of the data points by LSTM-WR fell between the upper and lower bounds. Also, at the maximum wind speed lower than 17.88 m/s (40 mph), which is the wind speed region of the training data, 95.4% of the data by LSTM-WR fell between the bounds. At the maximum wind speed higher than 17.88 m/s, 80% of the data points by LSTM-WR fell between the bounds.

$$f(x) = ae^{bx} + c \tag{6}$$

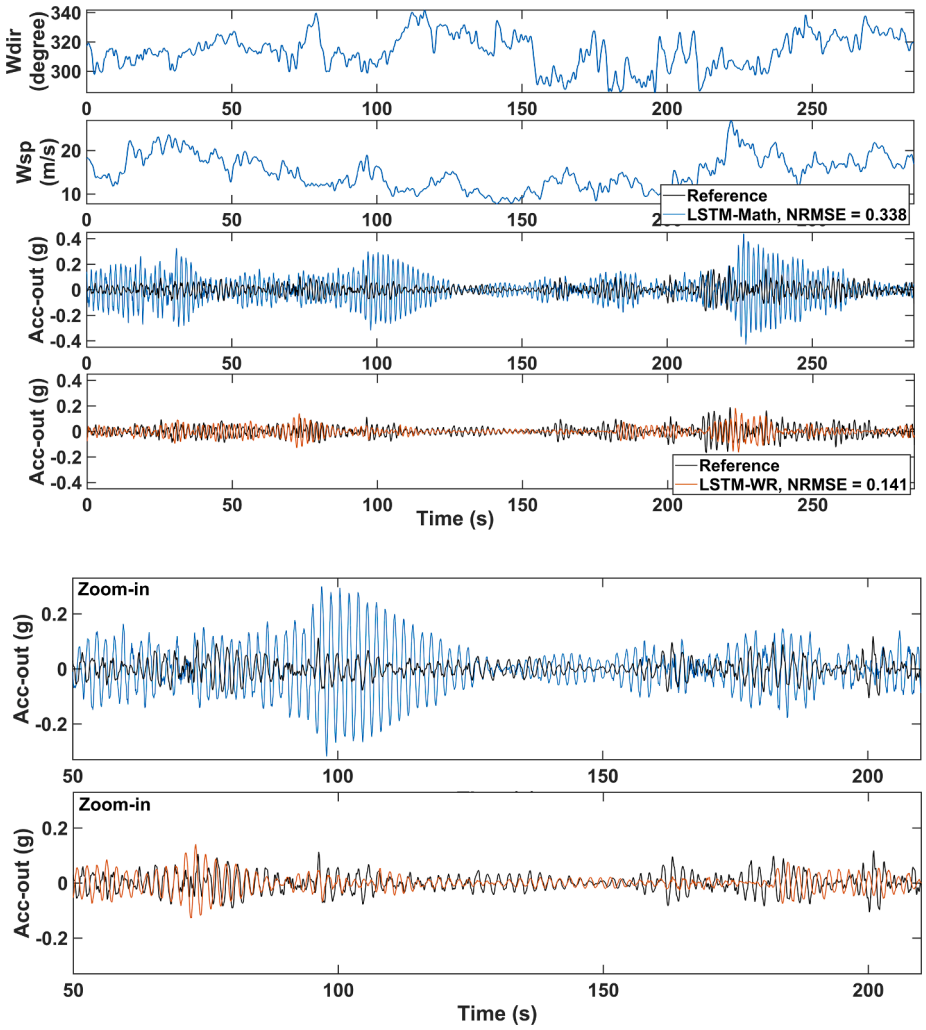

Fig. 16. LSTM-WR tested by a 5-min data in high wind condition.

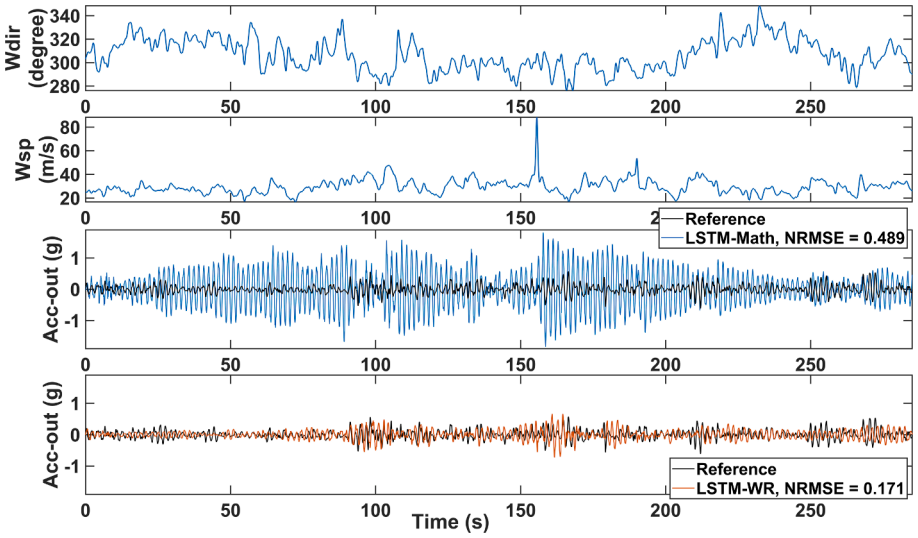

Fig. 17. LSTM-WR tested by a 5-min data in extreme wind condition.

5. Conclusions and discussions

The present study aims to develop a methodology to use machine learning techniques trained using monitoring data to predict the wind-induced response of a real-life flexible structure. The findings in this paper will be discussed and concluded in this section.

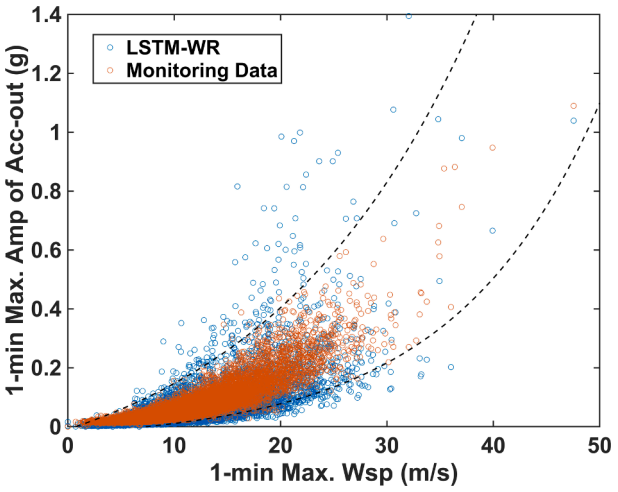

Fig. 18. 1-min maximum wind speed vs. 1-min maximum amplitude of out-of-plane acceleration.

A traffic signal structure in Ames, Iowa was monitored for more than a year. A mathematical model was derived and optimized. The proposed methodology then used two LSTM networks to accomplish predicting the wind-induced response of the traffic signal structure. The first LSTM network, LSTM-Math, was trained to replace the mathematical and to simulate wind-induced response more efficiently. The second LSTM network, LSTM-WR, was trained to correct the simulated response from LSTM-Math and to make better predictions of wind-induced response. Both LSTM networks played an important role on predicting wind-induced response. LSTM-Math provides general understanding of a structure and its wind-induced behavior, and LSTM-WR was trained to capture the informulable wind-induced behavior. Both LSTM networks were tested by unknown input data and their accuracies were evaluated.

Second, LSTM-Math was validated to be able to generate simulated wind-induced response quite close to the simulated response from the mathematical model. When comparing the computation times of the mathematical model and LSTM-Math, LSTM-Math was found to be more than 300 times faster. Therefore, this procedure can be applied to wind simulations on other structures to have higher efficiency. Also, reliability or fragility analysis on structures usually require large amounts of simulation data. By using this procedure, a trained LSTM network can reduce much time on running simulations.

Third, LSTM-WR was trained only by the monitoring data in regular wind condition and then tested by the unseen monitoring data in different wind conditions. The result showed LSTM-WR was able to correct the prediction from LSTM-Math and make closer prediction to the monitoring data. Although the prediction from LSTM-WR was not able to well match the monitoring data at every moment, it can well predict the acceleration amplitude even in high and extreme wind conditions. The monitoring data during the derecho of August, 2020 in Iowa was also used in testing LSTM-WR. It was found that LSTM-WR can predict acceleration amplitude and its predictions were more accurate compared to those of the LSTM-Math. It can be found in all different wind conditions that LSTM-Math, which is based on a physics-based models developed by traditional methods, generally provides conservative predictions, however, the error of the acceleration amplitude became quite large in high and extreme wind conditions. Therefore, the proposed method could bring a huge benefit in simulating wind-induced structural response when the targeting wind condition is beyond the limitation of the wind tunnel.

Finally, the proposed method requires only a few sensors to be installed on a structure in the field and the monitoring data in regular wind condition. When comparing to the traditional methods in developing an analytical model, the proposed method could be a cost-effective solution. It can be useful when simulating wind-induced structural response in a wide range of wind speeds and can be widely used on other structures suspected of having fatigue damage due to wind-induced vibrations.

CRediT authorship contribution statement

Li-Wei Tsai: Conceptualization, Methodology, Data curation, Software, Writing – original draft. **Alice Alipour:** Conceptualization, Supervision, Funding acquisition, Validation, Methodology.

Declaration of Competing Interest

The authors declare that they have no known competing financial interests or personal relationships that could have appeared to influence the work reported in this paper.

Acknowledgments

This paper is based on work supported by the Iowa Department of Transportation and National Cooperative Highway Research Program and National Science Foundation Award # 1751844. Their support is gratefully acknowledged. Any opinions, findings, and conclusions or recommendations expressed in this material are those of the authors and do not necessarily reflect the views of the funding agencies.

References

[1] AASHTO. LRFD specifications for structural supports for highway signs, luminaires, and traffic signals. In: Aashto; 2015. <https://doi.org/10.1016/B978-0-12-164491-8.50013-0>.
[2] Alipour A, Sarkar P, Tsai L-W, Jafari M. Development of a novel aerodynamic solution to mitigate large vibrations in traffic signal structures; 2020.
[3] Bani-Hani KA. Vibration control of wind-induced response of tall buildings with an active tuned mass damper using neural networks. Struct Control Health Moni: Off J Int Assoc Struct Control Monit Euro Assoc Control Struct 2007;14(1):83–108.
[4] Bengio Y, Simard P, Frasconi P. Learning long-term dependencies with gradient descent is difficult. IEEE Trans Neural Networks 1994;5(2):157–66.
[5] Castellon DF, Fenerci A, Øiseth O. A comparative study of wind-induced dynamic response models of long-span bridges using artificial neural networks, support vector regression and buffeting theory. J Wind Eng Ind Aerodyn 2021;209:104484.
[6] Chakraverty S, Marwala T, Gupta P, Tettey T. Response prediction of structural system subject to earthquake motions using artificial neural network. ArXiv Preprint ArXiv:0705.2235; 2007.
[7] Chen G, Wu J, Yu J, Dharani LR, Barker M. Fatigue assessment of traffic signal mast arms based on field test data under natural wind gusts. Transp Res Rec 2001;1770(1):188–94.
[8] Cruzado HJ, Letchford CW. Risk assessment model for wind-induced fatigue failure of cantilever traffic signal structures. Civil Eng. Ph.D. ; 2007. <https://doi.org/https://ttu-ir.tdl.org/ttu-ir/bitstream/handle/2346/9718/Cruzado_Hector_Diss.pdf>.
[9] Dexter RJ, Ricker MJ. NCHRP report 469: fatigue-resistant design of cantilevered signal, sign, and light supports. In: National Academy Press; 2002. <https://doi.org/10.17226/13746>.
[10] Ding J, Chen X, Zuo D, Hua J. Fatigue life assessment of traffic-signal support structures from an analytical approach and long-term vibration monitoring data. J Struct Eng 2016;142(6):4016017.
[11] Dongmei H, Shiqing H, Xuhui H, Xue Z. Prediction of wind loads on high-rise building using a BP neural network combined with POD. J Wind Eng Ind Aerodyn 2017;170:1–17.
[12] Florea MJ, Manuel L, Frank KH, Wood SL. Field tests and analytical studies of the dynamic behavior and the onset of galloping in traffic signal structures 2007; 7: 127.
[13] Frymoyer MC, Berman JW. Remaining life assessment of in-service luminaire support structures. Transportation Northwest (Organization); 2009.
[14] Goyal R, Dhonde H, Dawood M. Fatigue failure and cracking in high mast poles research project number 0-6650 October 2011 Department of Civil and Environmental Engineering University of Houston Houston , Texas. (January); 2012.
[15] Graves A, Mohamed A, Hinton G. In: Speech recognition with deep recurrent neural networks. Ieee; 2013. p. 6645–9.
[16] Hamilton III HR, Riggs GS, Puckett JA. Increased damping in cantilevered traffic signal structures. J Struct Eng 2000;126(4):530–7.
[17] Hareendran SP, Alipour A. Prediction of nonlinear structural response under wind loads using deep learning techniques. Appl Soft Comput 2022;129:109424.
[18] Hartnagel BA, Barker MG. Strain measurements on traffic signal mast arms. In: 1999 New Orleans Structures CongressStructural Engineering Institute of American

Society of Civil Engineers, Structural Association of Alabama, National Council of Structural Engineers Associations, Florida Structural Engineers Association, Louisiana Sect; 1999.
[19] Hochreiter S, Schmidhuber J. Long short-term memory. Neural Comput 1997;9(8):1735–80.
[20] Hu G, Kwok KCS. Predicting wind pressures around circular cylinders using machine learning techniques. J Wind Eng Ind Aerodyn 2020;198:104099.
[21] Jafari M, Sarkar PP, Alipour AA. A numerical simulation method in time domain to study wind-induced excitation of traffic signal structures and its mitigation. J Wind Eng Ind Aerodyn 2019;193:103965.
[22] Jozefowicz R, Zaremba W, Sutskever I. An empirical exploration of recurrent network architectures. International conference on machine learning 2015; 2342–2350. PMLR.
[23] Kaczinski MR, Dexter RJ, Van Dien JP. Fatigue-resistant design of cantilevered signal, sign and light supports, vol. 412. Transportation Research Board; 1998.
[24] Li S, Laima S, Li H. Cluster analysis of winds and wind-induced vibrations on a long-span bridge based on long-term field monitoring data. Eng Struct 2017;138:245–59.
[25] Li S, Laima S, Li H. Data-driven modeling of vortex-induced vibration of a long-span suspension bridge using decision tree learning and support vector regression. J Wind Eng Ind Aerodyn 2018;172:196–211.
[26] Li S, Li S, Laima S, Li H. Data-driven modeling of bridge buffeting in the time domain using long short-term memory network based on structural health monitoring. Struct Control Health Monitor 2021;28(8):e2772.
[27] Li T, Wu T, Liu Z. Nonlinear unsteady bridge aerodynamics: Reduced-order modeling based on deep LSTM networks. J Wind Eng Ind Aerodyn 2020;198:104116.
[28] Lim J, Kim S, Kim H-K. Using supervised learning techniques to automatically classify vortex-induced vibration in long-span bridges. J Wind Eng Ind Aerodyn 2022;221:104904.
[29] Lin P, Hu G, Li C, Li L, Xiao Y, Tse KT, et al. Machine learning-based prediction of crosswind vibrations of rectangular cylinders. J Wind Eng Ind Aerodyn 2021;211:104549.
[30] Martin J, Alipour A, Sarkar P. Fragility surfaces for multi-hazard analysis of suspension bridges under earthquakes and microbursts. Eng Struct 2019;197:109169.
[31] Micheli L, Hong J, Laflamme S, Alipour A. Surrogate models for high performance control systems in wind-excited tall buildings. Appl Soft Comput 2020;90:106133.
[32] Oh BK, Glisic B, Kim Y, Park HS. Convolutional neural network-based wind-induced response estimation model for tall buildings. Comput-Aid Civ Infrastruct Eng 2019;34(10):843–58.
[33] Oh BK, Glisic B, Park SW, Park HS. Neural network-based seismic response prediction model for building structures using artificial earthquakes. J Sound Vib 2020;468:115109.
[34] Perez-Ramirez CA, Amezquita-Sanchez JP, Valtierra-Rodriguez M, Adeli H, Dominguez-Gonzalez A, Romero-Troncoso RJ. Recurrent neural network model with Bayesian training and mutual information for response prediction of large buildings. Eng Struct 2019;178:603–15.
[35] Phares BM, Sarkar PP, Wipf TJ, Chang B. Development of fatigue design. procedures for slender, tapered support structures for highway signs, luminaries, and traffic signals subjected to wind-induced excitation from vortex shedding and buffeting. 132; 2007.
[36] Pino VA. Fatigue life prediction of cantilevered light pole structures fatigue life prediction of cantilevered light pole structures. (December); 2010.
[37] Puckett J, Ph D, Johnson R. Study of the effects of wind power and vortex-induced vibrations to establish fatigue design criteria for high – mast poles. (August); 2011.
[38] Pulipaka N, McDonald JR, Mehta KC. Wind effects on cantilevered traffic signal structures. Wind engineering retrospect and prospect: papers for the ninth international conference 1995 Volume IV. 1995.
[39] Pulipaka N, Sarkar PP, McDonald JR. On galloping vibration of traffic signal structures. J Wind Eng Ind Aerodyn 1998;77:327–36.
[40] Sezer OB, Ozbayoglu AM. Algorithmic financial trading with deep convolutional neural networks: time series to image conversion approach. Appl Soft Comput 2018;70:525–38.
[41] Sinh HN, Riedman M, Letchford C, O'Rourke M. Full-scale investigation of wind-induced vibrations of mast-arm traffic signal structures. New York (State): Dept. of Transportation; 2014.
[42] Tsai L-W, Alipour A. Assessment of fatigue life and reliability of high-mast luminaire structures. J Constr Steel Res 2020;170:106066.
[43] Tsai L-W, Alipour A. Studying the wind-induced vibrations of a traffic signal structure through long term health monitoring. Eng Struct 2021;247:112837.
[44] Tsai L-W, Dikshit S, Alipour A. Assessment of remaining life of high-mast luminaire structures. Structures Congress 2019: Bridges, Nonbuilding and Special Structures, and Nonstructural Components. American Society of Civil Engineers Reston, VA. pp. 329–339.
[45] Van Dien JP. Fatigue resistant design of cantivelered sign, signal, and luminaire support structures; 1995.
[46] Wang H, Wu T. Knowledge-enhanced deep learning for wind-induced nonlinear structural dynamic analysis. J Struct Eng 2020;146(11):4020235.
[47] Wieghaus KT, Hurlebaus S, Mander JB, Fry GT. Wind-induced traffic signal structure response: experiments and reduction via helical arm strakes. Eng Struct 2014;76:245–54. https://doi.org/10.1016/j.engstruct.2014.07.012.
[48] Wu J, Chen G, Barker MG. Wind-Induced Stresses on traffic signal mast arms: case studies; 2000.
[49] Xue J, Xiang Z, Ou Ge. Predicting single freestanding transmission tower time history response during complex wind input through a convolutional neural network based surrogate model. Eng Struct 2021;233:111859.
[50] Zhang R, Chen Z, Chen S, Zheng J, Büyüköztürk O, Sun H. Deep long short-term memory networks for nonlinear structural seismic response prediction. Comput Struct 2019;220:55–68.
[51] Zuo D, Letchford CW. Wind-induced vibration of a traffic-signal-support structure with cantilevered tapered circular mast arm. Eng Struct 2010;32(10):3171–9.
[52] Gholizadeh S, Salajegheh J, Salajegheh E. An intelligent neural system for predicting structural response subject to earthquakes. Advances in Engineering Software 2009;40(8):630–9.
[53] Lagaros N, Papadrakakis M. Neural network based prediction schemes of the non-linear seismic response of 3D buildings. Advances in Engineering Software 2012;44(1):92–115.
[54] Perera R, Sandercock S, Carnicero A. Civil structure condition assessment by a two-stage FE model update based on neural network enhanced power mode shapes and an adaptive roaming damage method. Engineering Structures 2020;207:110234.
[55] Ying W, Chong W, Hui L, Renda Z. Artificial neural network prediction for seismic response of bridge structure. 2009 International Conference on Artificial Intelligence and Computational Intelligence 2009;2:503–6.
[56] Micheli L, Cao L, Laflamme S, Alipour A. "Life cycle cost evaluation strategy for high performance control systems under uncertainties", ASCE. Journal of Engineering Mechanics 2020;146(2):1–15. 04019134.